Final Technical Report

Temporal Characteristics of Aftershock Sequences in the Intermountain West

USGS Award G20AP00028

Kristine L. Pankow
University of Utah
115 South 1460 East, Room 211 FASB
Salt Lake City. UT 84112-0102
Phone: 801-585-6274
Email: kris.pankow@utah.edu

Term: 1 January 2020 to 30 June 2021

This material is based upon work supported by the U.S. Geological Survey under Grant No. G20AP00028. The views and conclusions contained in this document are those of the authors and should not be interpreted as representing the opinions or policies of the U.S. Geological Survey. Mention of trade names or commercial products does not constitute their endorsement by the U.S. Geological Survey."

Abstract

Our work focuses on (i) producing aftershock model parameters for the eastern Intermountain West (IMW) region derived from the Reasenberg and Jones (1989) method, and (ii) investigating the sequences in three magnitude bins: M < 5, 5 ≤ M < 6, M ≥ 6. We test the hypothesis that earthquake sequences following large potentially surface-faulting earthquakes in the IMW behave fundamentally differently than those following moderate size earthquakes. To accomplish this, we compile catalogs of individual earthquake sequences using a pool of ~70,000 earthquakes recorded in Utah (University of Utah Seismograph Stations) and northwestern Montana (Montana Bureau of Mine and Geology). We apply and compare multiple declustering algorithms and develop quantitative criteria to discriminate mainshock-aftershock-like sequences from earthquake swarms, which are widespread in the IMW region. For the mainshock-aftershock-like sequences, we model the aftershock parameters, productivity and decay rate, and find that the new model, for M < 5 sequences, shows higher aftershock productivity than previously reported in the area. Last, we stacked the aftershock sequences from moderate earthquakes (5 ≤ M < 6), and the largest earthquakes (M ≥ 6) and proposed two additional sets of parameters based on the magnitude of the mainshock. The findings of our study can be used to inform and improve the reliability of USGS Operational Aftershock Forecasting, including an understanding of intersequence and geographic variability.

Report

Earthquake sequences

M < 5

For identifying earthquake sequences, we use the Utah catalog (1981-2016) (Bowman & Arabasz, 2007), which contains 26,305 earthquakes (-1.1 ≤ M ≤ 5.9), and the western Montana catalog (1981-2019, Montana Bureau of Mine and Geology) with 45,463 earthquakes (-0.9 ≤ M ≤ 5.8). We treat each catalog separately applying the same workflow and methodologies. First, we perform a thorough spatio-temporal analysis of the magnitude of completeness (M_{comp}), which is a crucial parameter to be determined prior to any statistical processing. For each catalog we calculate M_{comp} in a 0.1° x 0.1° grid using the maximum curvature method (Wiemer & Wyss, 2000) with a correction of 0.2. We then plot on a map the spatial distribution of the M_{comp} for the entire study period as well as for individual years, and several combinations, to test whether a spatial pattern exists. This analysis indicates that Utah can be divided into two sub-regions, namely south and north of 40.0° N. The western Montana catalog showed an almost constant M_{comp} throughout the study period. To determine temporal variability, we calculate the M_{comp} for each sub-catalog (northern Utah, southern Utah, western Montana) by applying a window of 150 events and a step of 5 to 50 (Fig. 1). This analysis indicates that the Utah sub-catalogs can be divided into two subperiods each, which coincide in time with the network expansion (Table 1). For Montana, we find three distinct sub-periods with M_{comp} decreasing with time (Table 1). Last, to confirm this variability we calculate M_{comp} for each year using the goodness of fit method (90-95%) (Wiemer & Wyss, 2000).

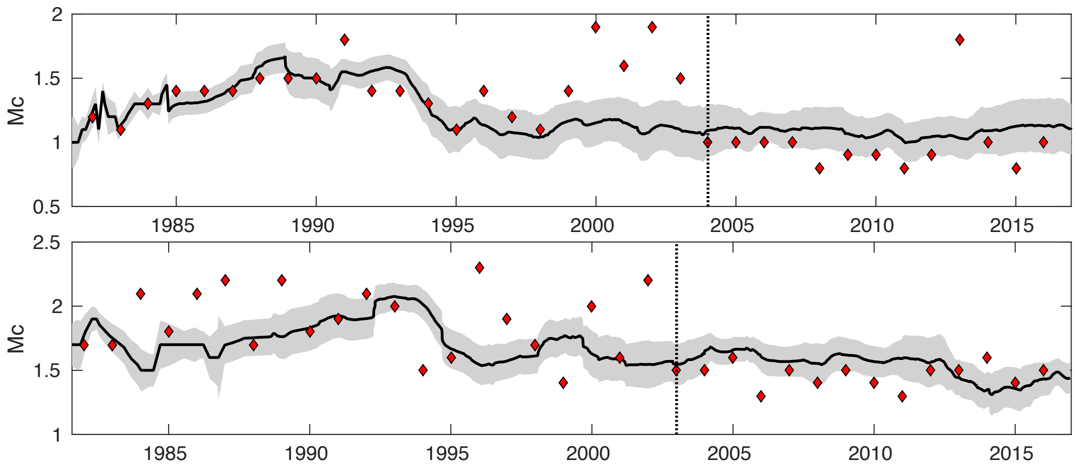

Figure 1 *Example of M_{comp} variability with time for (**top**) the northern, and (**bottom**) southern Utah.*

Table 1 *Sub-catalogs along with magnitude of completeness (M_{comp}), number of earthquakes raw catalog ($N_{original}$), number of earthquakes complete catalog ($N_{complete}$).*

Subarea & Subperiod	M_{comp}	$N_{original}$	$N_{complete}$
Northern Utah 1981-2003	1.4	8445	3747
Northern Utah 2004-2016	1.0	4590	2595
Southern Utah 1981-2002	2.1	6752	1882
Southern Utah 2003-2016	1.5	6518	3270
Western Montana 1982-1987	2.3	4009	793
Western Montana 1988-2000	1.3	8662	4806
Western Montana 2001-2019	1.0	30371	17502

The next step of our analysis concerns the identification of earthquake sequences for each sub-catalog. At this stage the earthquake sequences are not classified into different types rather identified as earthquake clusters in general. We applied three declustering algorithms (Jacobs et al., 2013; Reasenberg, 1985; Zaliapin & Ben-Zion, 2013; Zaliapin et al., 2008) and looked at the interevent distribution of the earthquakes in the declustered catalog to select the optimal set of parameters. Table 2 summarizes the results for each sub-catalog and algorithm.

To classify earthquake sequences into mainshock-aftershock sequences and earthquake swarms we calculate the skewness of moment release history for each sequence (e.g. Chen & Shearer, 2011; Mesimeri et al., 2019; Roland & McGuire, 2009). We then examine the distribution of skewness for each sequence in each sub-catalog to identify bimodality, which provides a discrimination between the different types of sequences. An example is shown in Figure 2, where a change in the slope defines a change between swarms and mainshock-aftershock sequences. Applying this discriminant to each sub-catalog and declustering algorithm resulted in a variability on earthquake sequence type characterization, strongly dependent on the declustering method used.

The final earthquake sequence selection is performed by summarizing the results of each declustering method. In detail, we first group commonly identified earthquake sequences identified by all three declustering methods. Then, we characterize a sequence as a mainshock-aftershock type if at least two of the declustering algorithms agree on the sequence type. Figure 3 shows the final selection of mainshock-aftershock sequences for Utah (20) and western Montana (11). We then apply the Reasenberg & Jones (1989) model to define the α, p, and c parameters for each sequence. As we used multiple declustering methods we first calculate the parameters for each sequence identified by each declustering method and then calculate the median value for each declustering method. The final values are the average parameters from each declustering method (Table 3).

Table 2 *Summary of the declustering results for the thrre algorithms used in this study. RSB85* (P. Reasenberg, 1985)*, CURATE* (Jacobs et al., 2013)*, NN* (Zaliapin & Ben-Zion, 2013)

		RSB85			CURATE			NN		
Subarea & Subperiod	**N_{comp}**	**N_{declus}**	**N_{clus}**	**Clusters N≥10**	**N_{declus}**	**N_{clus}**	**Clusters N≥10**	**N_{declus}**	**N_{clus}**	**Clusters N≥10**
Northern Utah 1981-2003	3747	2733	1303	18	2411	1686	18	2001	2142	24
Northern Utah 2004-2016	2595	2007	791	15	1821	1070	14	1553	1367	22
Southern Utah 1981-2002	1882	1294	727	12	1174	892	17	1020	1037	21
Southern Utah 2003-2016	3270	2298	1226	27	2117	1460	29	1743	1873	37
Western Montana 1982-1987	793	578	262	3	499	374	5	425	450	4
Western Montana 1988-2000	4806	3899	1190	14	3546	1708	19	2971	2359	33
Western Montana 2001-2019	17502	11,355	7188	71	10,960	8554	111	8345	10,540	98

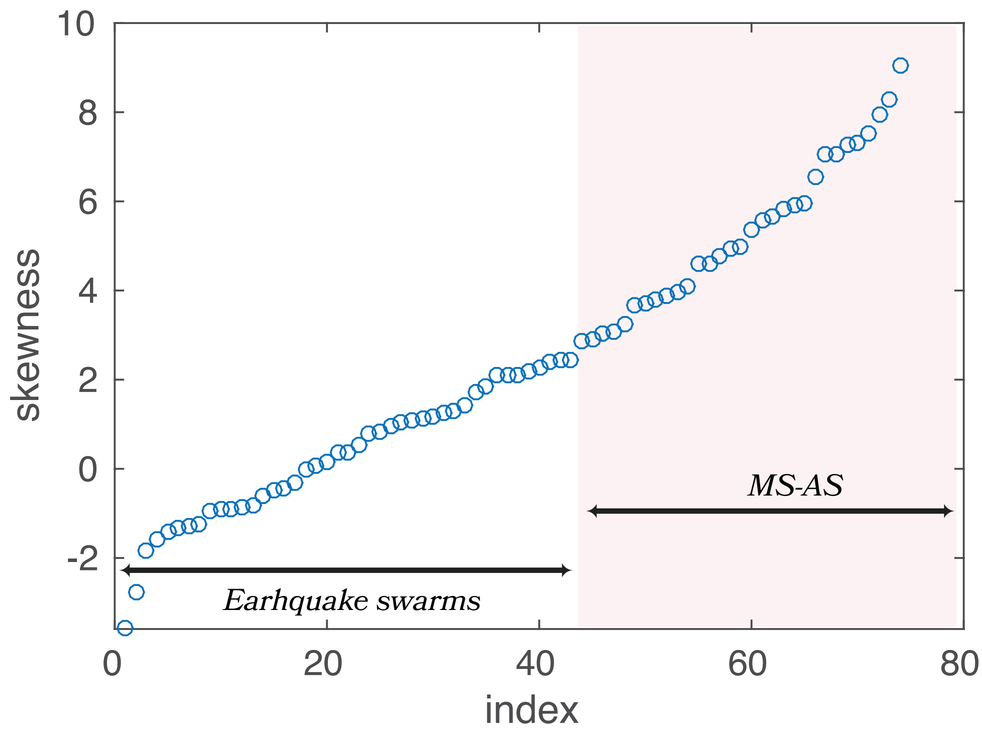

Figure 2 Sorted values of skewness of moment release history.

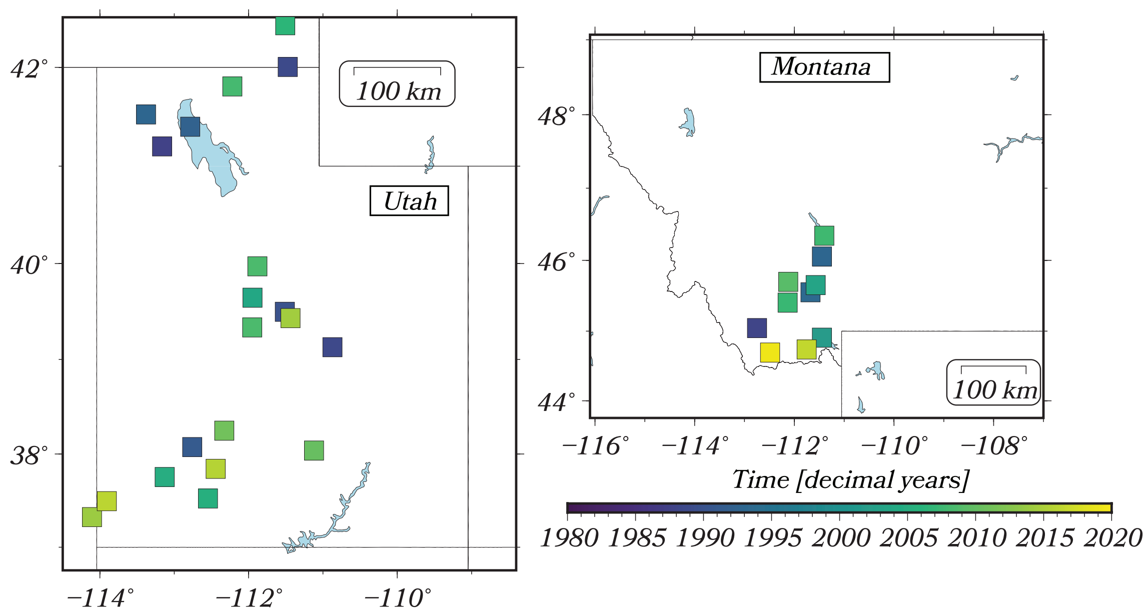

Figure 3 Mainshock- aftershock seqeunces in (**left**) Utah, and (**right**) western Montana. Squares show the mean seqeunce epicenter color-coded by time of occurrence.

5 ≤ M < 6

For earthquake sequences that have a maximum magnitude between 5 and 6 we used a different approach. The current dataset contains five typical mainshock–aftershock sequences in this magnitude range, namely the 2008 Wells, NV (M 5.9), the 2020 Magna, UT (M 5.7), the 2005 Dillon, MT (M 5.6), the 2017 Lincoln, Montana (M 5.8), and the 2016 Hoback, Wyoming (M 4.8) earthquakes. We combined these sequences into one catalog, calculate the magnitude of completeness (M_{comp}=2.6), and find a b-value equal to 0.8. Then, we estimate the model parameters for the stacked sequences (Table 3).

M ≥ 6

We perform a similar analysis (combining multiple events) for the 1959 Hebgen Lake, MT (M 7.2), 1983 Borah Peak, ID (M 7.3), and 2020 Stanley, ID (M 6.5). The magnitude of completeness for these three events is 3.6 and we select a b-value equal to 1 (Table 3).

Table 3 Parameters for Operational Afterschok Forecasting proposed in this study for different magnitudes.

Magnitude range	M_{eqv}	M_{comp}	alpha	p	c
M < 5	variable	variable	-1.37	1.01	0.04
5 ≤ M < 6	5.8	2.6	-0.77	0.75	0.005
M ≥ 6	6.5	3.6	-1.64	0.84	0.13

ETAS Modeling

Here we report our attempt to model the typical mainshock-aftershock sequences using the ETAS model (Ogata, 1988). Due to the very few events, especially in the cases of the 1959 Hebgen Lake, MT and 1983 Borah Peak, ID, it was difficult to estimate the model parameters and the results are inconclusive. Thus, we do not include this analysis in this report.

Proposed model

To summarize, we propose a new model for the eastern Intermountain West that could be used in the USGS Operational Aftershock Forecasting. The new model depends on the magnitude of the mainshock, and therefore consists of three different magnitude bins and sets of parameters. For mainshocks with M < 5 (blue line, Fig. 4) we observe a higher productivity than proposed by the Generic Utah model, the California model (Reasenberg & Jones, 1989), and the shallow continental active nonsubduction region model (ANSR-SHALCON) (Page et al., 2016). The model for mainshocks between 5 ≤ M < 6 (red line, Fig. 4 left panel), shows that these earthquake sequences are more productive and prolonged in time than the smaller magnitude events. In contrast, aftershock sequences for M > 6 (red line, Fig. 4 right panel) are less productive.

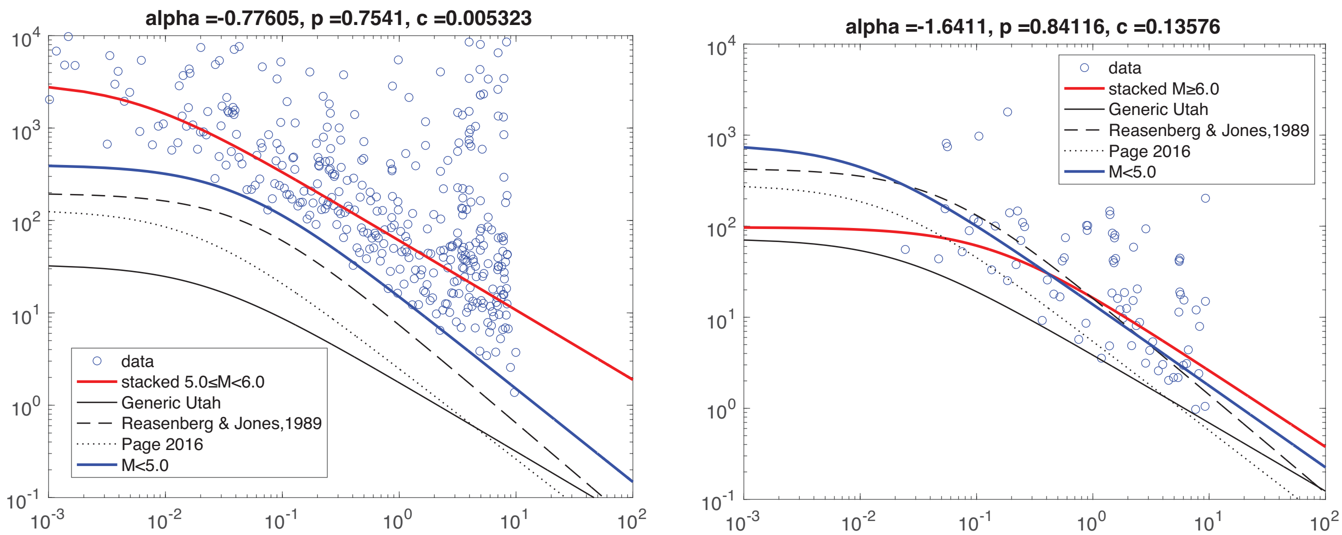

Figure 4 New model for Intermountain West, (**left**) for 5.0≤M<6.0 sequences with M_{max}=5.8, M_{comp}=2.6, and bval=0.8, (**right**) for M≥6.0 sequences with M_{max}=6.5, M_{comp}=3.6, bval=1. Blue line shows the proposed model for sequences with M<5.0.

References

Bowman, S. D., & Arabasz, W. J., (2017). Utah Earthquakes (1850-2016) and Quaternary Faults, *Utah Geological Survey Map 277.*

Chen, X., & Shearer, P. M. (2011). Comprehensive analysis of earthquake source spectra and swarms in the Salton Trough, California. *Journal of Geophysical Research B: Solid Earth*, *116*(B09), doi:10.1029/2011JB008263. Retrieved from http://www.scopus.com/inward/record.url?eid=2-s2.0-80053311148&partnerID=40&md5=28cea561d93baadb0a277025e71406b7

Jacobs, K. M., Smith, E. G. C., Savage, M. K., & Zhuang, J. (2013). Cumulative rate analysis (CURATE): A clustering algorithm for swarm dominated catalogs. *Journal of Geophysical Research: Solid Earth*, *118*(2), 553–569. https://doi.org/10.1029/2012JB009222

Mesimeri, M., Karakostas, V., Papadimitriou, E., & Tsaklidis, G. (2019). Characteristics of earthquake clusters: Application to western Corinth Gulf (Greece). *Tectonophysics*, 228160. https://doi.org/10.1016/j.tecto.2019.228160

Ogata, Y. (1988). Statistical Models for Earthquake Occurences and Residual Analysis for Point Processes. *Journal of the American Statistical Association*, *83*(401), 9–27.

Page, M. T., van Der Elst, N., Hardebeck, J., Felzer, K., & Michael, A. J. (2016). Three ingredients for improved global aftershock forecasts: Tectonic region, time-dependent catalog incompleteness, and intersequence variability. *Bulletin of the Seismological Society of*

America, *106*(5), 2290–2301. https://doi.org/10.1785/0120160073

Reasenberg, P. (1985). Second-Order Moment of Central California Seismicity, 1969-1982. *Journal of Geophysical Research*, *90*(B7), 5479–5495.

Reasenberg, P. A., & Jones, L. M. (1989). Earthquake hazard after a mainshock in California. *Science*, *243*, 1173–1176. https://doi.org/10.1038/374492b0

Roland, E., & McGuire, J. J. (2009). Earthquake swarms on transform faults. *Geophysical Journal International*, *178*(3), 1677–1690. https://doi.org/10.1111/j.1365-246X.2009.04214.x

Wiemer, S., & Wyss, M. (2000). Minimum magnitude of completeness in earthquake catalogs: Examples from Alaska, the Western United States, and Japan. *Bulletin of the Seismological Society of America*, *90*(4), 859–869. https://doi.org/10.1785/0119990114

Zaliapin, Ilya, & Ben-Zion, Y. (2013). Earthquake clusters in southern California I: Identification and stability. *Journal of Geophysical Research: Solid Earth*, *118*(6), 2847–2864. https://doi.org/10.1002/jgrb.50179

Zaliapin, Ilyar, Gabrielov, A., Keilis-Borok, V., & Wong, H. (2008). Clustering analysis of seismicity and aftershock identification. *Physical Review Letters*, *101*(1), 4–7. https://doi.org/10.1103/PhysRevLett.101.018501

Project Data

The Utah catalog is available at https://quake.utah.edu/earthquake-information-products/earthquake-catalogs/utah-earthquake-map-catalog. For the western Montana we use the ANSS Comprehensive Earthquake Catalog (ComCat) available at https://earthquake.usgs.gov/earthquakes/search/.

Bibliography

Mesimeri M. & Pankow K.L (2020), On earthquake sequences in the Intermountain West, S038-0004 presented at 2020 AGU Fall Meeting, 1-17 Dec.

Mesimeri M. & Pankow K.L (2021), Revisiting operational aftershock forecasting in the Intermountain West, *in preparation for submission in Seismological Research Letters*.

Acknowledgments of Support and Disclaimer

This material is based upon work supported by the U.S. Geological Survey under Grant No. G20AP00028. The views and conclusions contained in this document are those of the authors and should not be interpreted as representing the opinions or policies of the U.S. Geological Survey. Mention of trade names or commercial products does not constitute their endorsement by the U.S. Geological Survey."